

Article

Enzyme Immobilization on Stainless Steel Fleece and Its Mass Transfer Enhancement of Enzymatic Catalysis in a Rotating Packed Bed Reactor

Ruiyi Yang ^{1,†}, Juntao Xu ^{1,2,†}, Jinglong Wu ¹, Dong Lu ¹, Fang Wang ¹ and Kaili Nie ^{1,*} 

¹ Beijing Key Laboratory of Bioprocess, National Energy R&D Center for Biorefinery, College of Life Science and Technology, Beijing University of Chemical Technology, Beijing 100029, China; xu_juntao1904@163.com (J.X.); 2021400300@mail.buct.edu.cn (D.L.)

² Sinovac Life Sciences Co., Ltd., Beijing 102600, China

* Correspondence: niekl@mail.buct.edu.cn

[†] These authors contributed equally to this work.

Abstract: Rotating packed beds (RPB) facilitate the mixing of heterogeneous substrates, and promote high mass transfer efficiency in heterogeneous reactions. For the enzymatic reactions, traditional porous particles with immobilized enzymes are sensitive to the strong shear force of the RPB, thus limiting its application. This work offers a strategy for enzyme immobilization on the surface of stainless-steel fleece, to improve the shear strength resistance of immobilized enzymes. Lipase was applied to investigate and optimize the immobilization. Finally, a fatty acid hydratase (FAH) was applied for immobilization based on the optimized method, which was further applied for evaluating its performance in RPB. The results indicated that metal immobilized enzymes resist a higher shear force than their particle-immobilized alternatives. Operating at a centrifugal force factor (β) of 30, the hydration conversion rate of 96% is achieved after 8 h, which was from nearly 38% faster than in a stirrer tank reactor (hydration yield of 60%). The metal immobilization, moreover, efficiently improved the enzyme reusability, as demonstrated by a conversion rate remaining above 90% after 15 batches. These results indicated that a metal immobilization method combined with an RPB reactor significantly increases the efficiency of enzymatic reactions.

Keywords: rotating packed bed; immobilization; heterogeneous reaction; mass transfer enhancement; hydration



Citation: Yang, R.; Xu, J.; Wu, J.; Lu, D.; Wang, F.; Nie, K. Enzyme Immobilization on Stainless Steel Fleece and Its Mass Transfer Enhancement of Enzymatic Catalysis in a Rotating Packed Bed Reactor. *Catalysts* **2023**, *13*, 1501. <https://doi.org/10.3390/catal13121501>

Academic Editor: B. Lesiak-Orłowska

Received: 30 October 2023

Revised: 30 November 2023

Accepted: 5 December 2023

Published: 8 December 2023



Copyright: © 2023 by the authors. Licensee MDPI, Basel, Switzerland. This article is an open access article distributed under the terms and conditions of the Creative Commons Attribution (CC BY) license (<https://creativecommons.org/licenses/by/4.0/>).

1. Introduction

Facing a fossil energy crisis, new energy sources have gained widespread attention in the past decades, and the role of the green industry for social development is constantly increasing [1,2]. Bio-catalysis is developing as an alternative to traditional chemical processes, and will further contribute to the development of green industries and clean production methods. Immobilization was a traditional operation for improving the stability and reusability of enzymes. Most immobilization procedures do not actively control the configuration of the enzymes, resulting in the inevitable burying and inaccessibility of their active site. Enzymes undergo substantial changes in the surface microenvironment, conformation, and protein refolding following an immobilization process [3,4]. In the process of enzyme application, it was found that mass transfer between immobilized enzymes and substrates largely affected the reaction efficiency, especially for the heterogeneous reactions in water-oil [5] or water-gas systems [6]. For the conventional chemical catalytic process, this problem could be improved through increasing the stirring speed [7] or introducing mass transfer enhancement aids [8].

In the view of the mass transfer for heterogeneous reactions, the common problems are the slow diffusion rate of the reactants on the boundary layer of different phases.

Additionally, insufficient mixing would result in concentration gradients of degradation products in the reaction system. Both problems would lead to a slow reaction rate. Normally, the strategies of mass transfer enhancement between the different phases, like the application of an RPB reactor would enhance the reaction rate and the efficiency of heterogeneous reactions. However, compared to the chemical catalysts, as a natural protein, enzymes are very sensitive to the shear force, since a strong shear force derived from mass transfer enhancement method would denature the enzymes. How to improve the shear strength resistance of enzymes was the main problem for the application of RPB on enzymatic catalysis.

Hydration of unsaturated fatty acids is a typical heterogeneous reaction with water-oil as two immiscible phases. The product of hydration, 10-hydroxy-12-octadecenoic acid (10-HOA), was a typical hydroxy-unsaturated fatty acid which would derive from microbes naturally. It has been reported that 10-HOA has a good fungal inhibition effect, which is excellent when added to fermented bread. It has potential regulatory and controlling effects on brain inflammation, and animal experiments have found that 10-HOA can also effectively prevent allergic dermatitis. 10-HOA has great potential for application in food and biomedical fields, and its efficient preparation is of great significance. As a biocatalyst, fatty acid hydratase (FAH) can generate secondary and tertiary alcohols by asymmetric addition of H₂O to the Δ^9 double bond of unsaturated fatty acid [9]. By using such a method, extremely high carbon utilization can be achieved in the production of hydroxy fatty acid (HFA) without the need for expensive co-factors (NADPH/NADH). Therefore, FAH is a key enzyme for the preparation of HFA by modification of unsaturated fatty acids.

FAH has many advantages, but the efficiency of the hydration can be limited by the low oil-water interface mass transfer rate. Also, traditional stirred reactors would lead to low biocatalytic efficiency, low yields, and long-lasting time consumption. Therefore, the application of a mass transfer enhancement technology is an important target for the enzymatic hydration process. The rotating packed bed (RPB) mass transfer enhancement reactor contributes to solving the disadvantages mentioned above. When the substrates flow into the packing of the RPB, the rotation accelerates the liquid through the screen packing within a short range, increasing the contact area of the interfacial reaction through the collision between the high-speed packing and the liquid substrate, thus effectively improving the process transfer efficiency [10]. Meanwhile, high-speed rotation of liquid reactants will create a huge interphase contact area, uniform mixing degree, and enhancement of the mass transfer efficiency [11,12].

RPB has been proved instrumental in providing a beneficial environment for the controlled synthesis of nanocomposites [13]. In polymer synthesis [14], RPBs have been successfully applied to optimize reaction conditions, enhance mixing efficiency, and improve heat transfer. For decolorization processes, RPB has demonstrated effectiveness in removing colorants from various substances [9]. Furthermore, RPB enhanced the reaction rates, resulting in an improvement of biodiesel yield and quality [13]. Research about its application for biocatalytic processes has also been reported [15], although the rotation speed for the biocatalytic process was significantly lower than that in a chemical process in view of the weak shear strength resistance of the enzyme. Common immobilization with porous carriers could protect enzymes from damage of the shear, but it would reduce the mass transfer due to the diffusion resistance in the micro-channels of the carrier. Thus, new immobilization strategies to enhance the shear strength resistance and accelerated mass transfer diffusion of the RPB application could jointly promote the biocatalytic process.

Furthermore, normally the packing of the RPB was a stainless-steel fleece, if the enzyme would be immobilized on the packing fleece, the biocatalyst would be better distributed for the RPB reaction process. However, when the stainless-steel fleece acted as the carrier, with the rigidity of stainless-steel, the enzyme would be more stable, to benefit for the shear strength resistance of enzyme. Minier et al. [16] provided a method of grafting of primary amines by aminosilanization of oxidized stainless steel, then cross-linking of glycosidase lysozyme on the pretreated surface with glutaraldehyde as a cross-linking

agent. This method has successfully immobilized protein on the surface of metals material. This work indicated that the enzyme could be immobilized on the metal surface through cross-linking. However, the capacity of the metal is a problem for the immobilization.

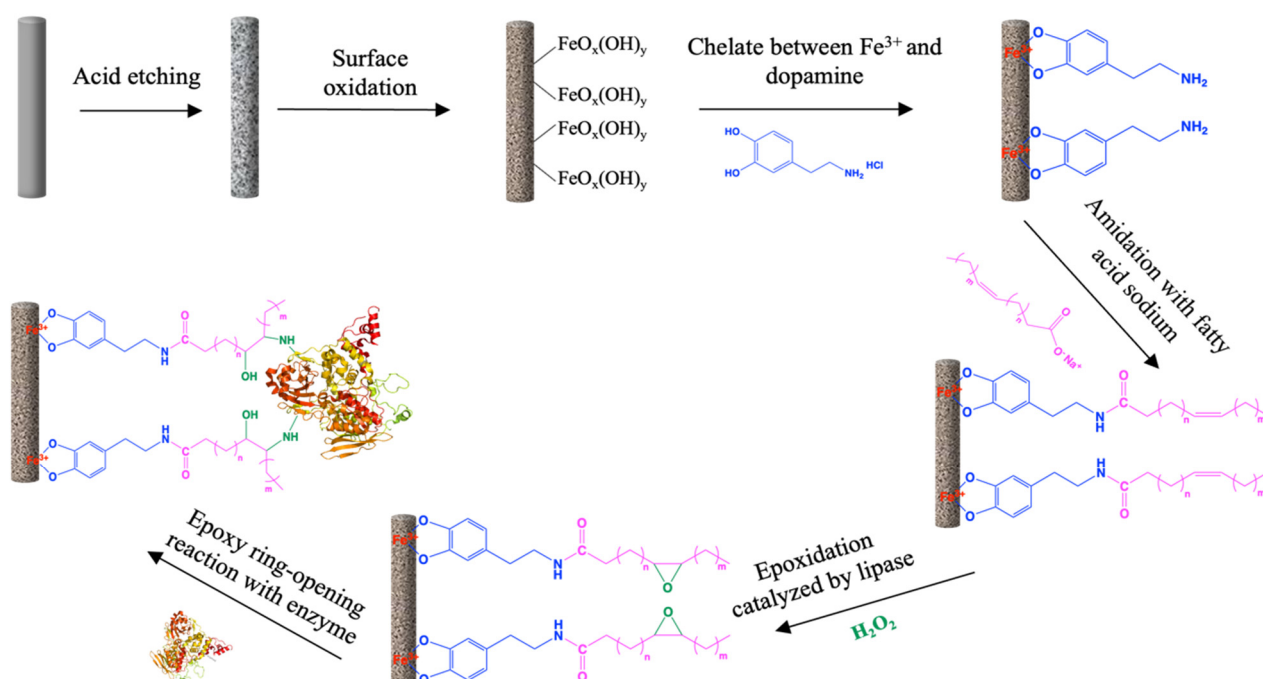
Based on the problems mentioned above, a strategy with a nearly monolayer enzyme immobilization on a stainless-steel surface was developed, whereby the enzyme could be immobilized on the metal mesh rotor of the RPB. A commercial free lipase, CALB, was applied for the optimization of the immobilization process, and heterogeneous reactions of unsaturated fatty acid hydration catalyzed by FAH were used to validate the performance of this immobilization method applied in the RPB reactor. Furthermore, the operation parameters of this new RPB with immobilized hydratase were optimized, and the effect of mass transfer enhancement of this RPB was also evaluated.

2. Results and Discussion

Compared to nanoscale carriers, which offer large surface areas to load more enzymes [17], and with the size effect of nanoparticles, the mass transfer resistance would be reduced for the reaction [18]. However, the weak shear strength resistance property of the enzymes was not greatly improved, and the particle type of the immobilized enzymes was still difficult to apply on the RPB [15]. The mass transfer enhancement function of the RPB reactor is mainly realized by the internal rotor and packing layer. At the beginning, the substrate liquid was vertically injected into the rotor through the distributor. With the centrifugal force, the liquid would knock on the packing layer and tear into fine droplets, which would greatly improve the specific surface area of the substrate liquid and reduce the surface tension [19]. From our earlier research, it was found that when the traditional particle-immobilized enzymes were applied in the RPB, due to the fragile structure of the immobilization carrier, the strong shear-force from the impact between particles and packing net would break the immobilized carrier, resulting in enzyme damage [15]. If the enzyme could be strongly immobilized on the surface of the packing layer, it could provide a significant surface area for the reacting liquid and act as a catalyst on the packing layer. These objectives led to developing a method of enzyme immobilization on the surface of stainless steel mesh.

2.1. Schematic Design for the Enzyme Immobilization on the Surface of Stainless-Steel

The mechanism of immobilization was based on the chelate reaction between Fe^{3+} and the hydroxy group of dopamine. The whole process (Scheme 1) includes six steps. Initially, cleaned stainless steel was etched with HCl to increase the surface area of the metal. Due to the hydroxy groups, dopamine could chelate with Fe^{3+} after roughening the metal through oxidation. Afterwards, the free amino group of dopamine was amidated with the unsaturated fatty acid under the catalysis of 4-(4,6-Dimethoxy-1,3,5-triazin-2-yl)-4-methylmorpholinium chloride (DMT-MM). The unsaturated double bonds of fatty acids were subsequently epoxidated under the mild conditions catalyzed by lipase. Finally, based on the property of the amino group, this would cause an automatically epoxy ring-opening reaction under the mild condition with ambient temperature [19]. The enzymes were covalently immobilized on the surface of the metal through the epoxy ring-opening reaction from the amino group on its surface residues. To investigate different aspects of this process on the efficiency of immobilization, CALB lipase was used as the immobilized enzyme and its catalytic ability and reuse ability for the esterification reaction of lauric acid and octanol was used as a readout.



Scheme 1. Steps of enzyme immobilized on the surface of stainless steel.

2.1.1. Influence of Different Oxidation Methods on the Immobilization

The surface of the stainless-steel net was smooth after being cleaned with NaOH and ethanol; its low surface area was not suitable for immobilization. HCl, with a concentration of 0.5 M, was used for etching for 12 h to successfully increase its surface area. However, the exposed zero-valent Fe element was hard to chelate with dopamine. Compared with the zero-valent Fe, the oxidation product of $\text{FeO}_x(\text{OH})_y$ has a better chelate ability. To investigate the effect of metal oxidation on the immobilization, CALB lipase was applied, and the catalytic ability and reusability of the immobilized lipase for the esterification of lauric acid and octanol was monitored.

Firstly, the oxidation effects of H_2O_2 and KMnO_4 were compared. From the catalytic results of the immobilized lipase (Figure 1a), it could be found that both of the two oxidizing agents had a similar effect for the following chelate reaction and immobilization, and the oxidation treatment would greatly benefit the catalytic ability of the immobilized enzyme compared to the non-oxidized supports. The treatment with KMnO_4 was easier to perform than that of H_2O_2 . The concentration and operation time of the KMnO_4 oxidation was further optimized. The results of Figure 1b illustrated that the concentrations of KMnO_4 were above 1 mM, and the oxidation time longer than 1 h had similar effects for immobilization. However, from the results of Figure 1c, it is clear that the concentration of KMnO_4 mainly influenced the reusability of the immobilized enzyme. Higher concentrations would lead to more $\text{FeO}_x(\text{OH})_y$ on the surface of stainless-steel, which would chelate with dopamine, and provide more grafting points for further immobilization.

2.1.2. Influence of Dopamine Dosage on the Immobilization

The chelation between Fe^{3+} and dopamine was the basis of the whole immobilization of Scheme 1. As the basis of the chelation, the contents of Fe^{3+} depends on the oxidation reaction on the surface of the carrier metal. The dosage of dopamine also affected the number of amino groups existing on the metal surface after coordination. From the esterification yields of metal-immobilized lipase with different dosage of dopamine (Figure 2), a minimum 2 mg/L dosage of dopamine is needed. Higher dosages do not enhance the catalytic ability and reusability of immobilized lipase.

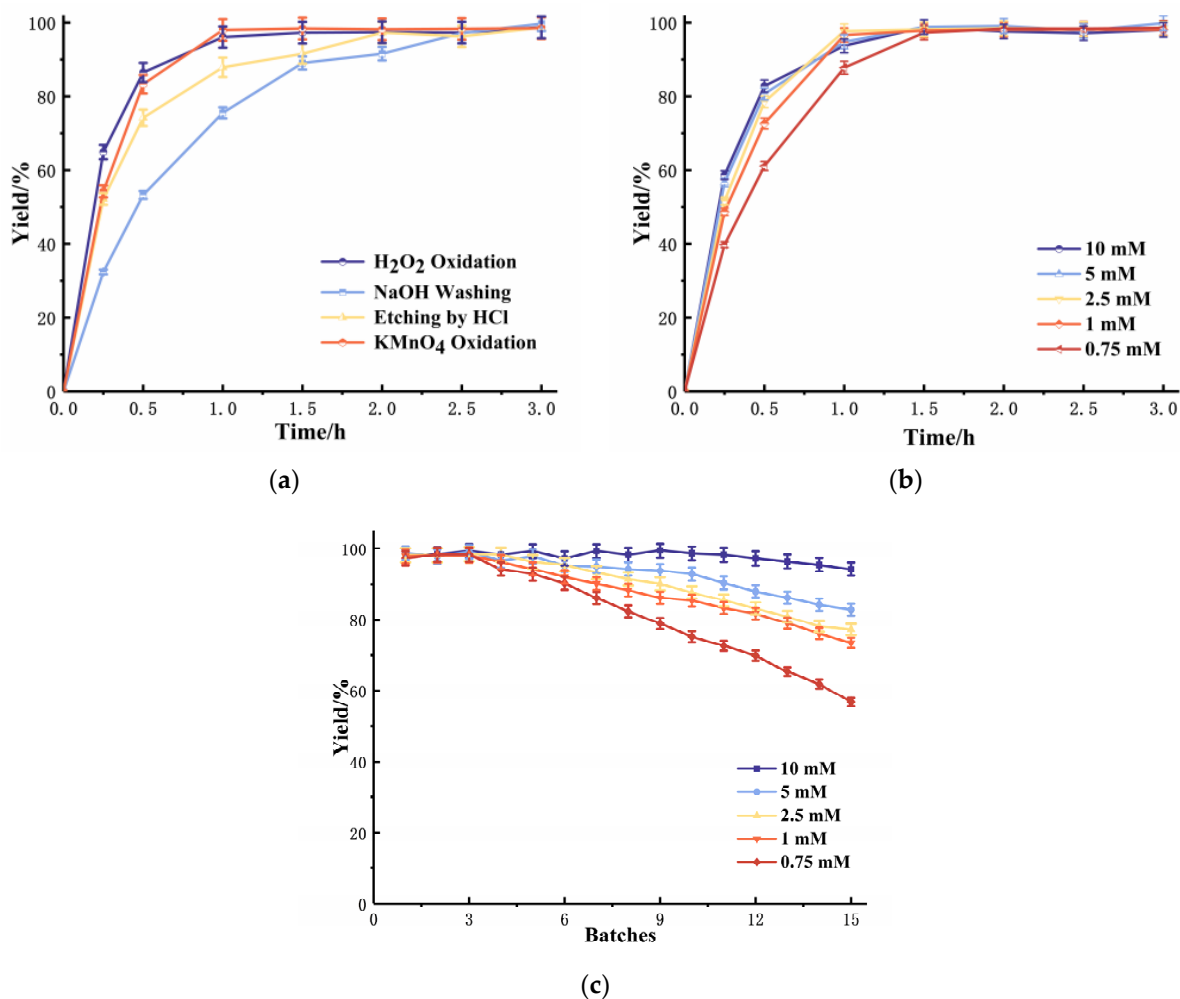


Figure 1. Different oxidation methods on the immobilization of lipase. (a) Yields of lipase under different optimized treatments (b) KMnO₄ loading and duration on the catalytic ability of immobilized enzymes (c)The reusability of immobilized enzyme under different concentrations of KMnO₄.

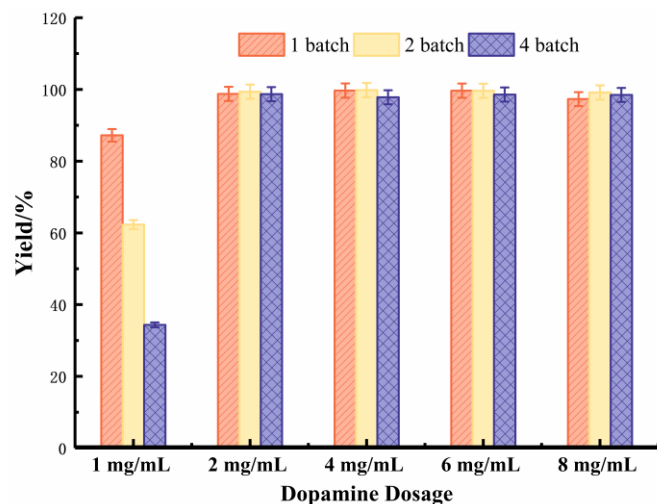


Figure 2. Effect of Dopamine dosage on the immobilization of lipase under different batches.

2.1.3. Influence of Unsaturated Organic Acids on the Immobilization

Organic acids (acrylic acid and fatty acids) have two functions in the immobilization process. On one side, they act as a linker, which increases the distance between enzyme

molecules and the surface of the carrier, thus improving the flexibility of enzyme molecules dispersed on the carrier surface. On the other side, they provide the epoxidation reaction sites, which were applied for further covalently immobilization of the enzyme. The results of the 1 h reaction contains comparison of different organic acids (Figure 3a) indicating that the acrylic acid is not suitable, which might be due to its chain length being too short. When the enzyme molecules are linked on the surface, the short chain linker is not flexible, and the steric hindrance between the enzyme molecules is large, which is not conducive to the distribution of enzyme molecules. Compared to other fatty acids, the double bond for 9-decenoic acid is in the end of an alkyl chain of the carboxylic acid. The results of Figure 3a indicated that the alkyl chain after a double bond would benefit the immobilization. This may be attributed to the hydrophobic alkyl chain regulating the surface properties of the carrier and making it fit for stabilization of the enzyme molecular conformation. Because the double bonds for oleic and linoleic acid are further from the carboxylic acid, therefore providing less steric hindrance to the metal surface, this may be the reason for the increased activity of the immobilized enzyme produced from these two fatty acids. For the two kinds of octadecane acids, linoleic acid has one more double bond than oleic acid, which may provide more covalent bonds with the enzyme, thus stabilizing it.

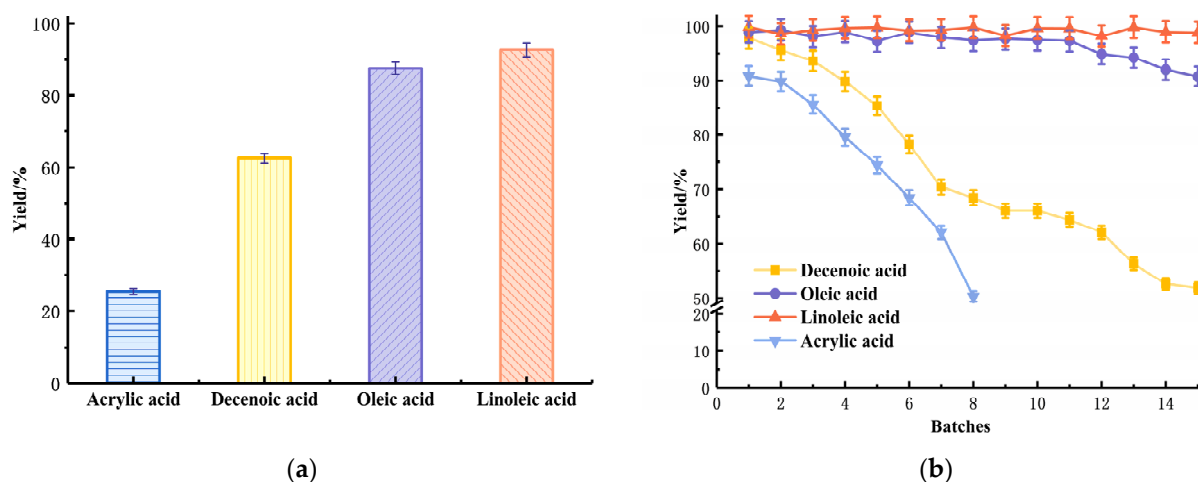


Figure 3. Influence of unsaturated organic acids on the immobilization catalyzed by lipase; (a) The catalytic ability of a different linker immobilized by lipase, 1 h reaction; (b) The immobilized enzyme reusability under a different linker, 3 h for each batch.

Meanwhile, the results of Figure 3b (3 h reaction for each batch) illustrated the reusability of metal-immobilized lipase with four kinds of organic acid linker. When the equilibrium time of enzymatic reaction was 3 h, the esterification yield of the immobilized enzymes with linoleic acid grafted as a linker remained above 95% after 15 batches of reaction.

2.1.4. Immobilization of Enzymes

The immobilization of enzymes is based on the epoxy ring-opening reaction of amino groups from the surface of the enzyme and the epoxy group in the unsaturated acids. For traditional Prileshajev-epoxidation, H_2O_2 was applied as an oxygen donor while formic acid was applied for the formation of peroxy-acid, and a small amount of inorganic acid was generally added to increase the epoxidation rate [20]. However, the usage of inorganic acid would destroy the chelate bonds of Fe^{3+} and dopamine, as well as cause the side reaction of epoxy ring-opening by water, thus influencing the immobilization of the enzyme on the surface of the metal. These problems prevent applying the traditional epoxidation method for the immobilization in this work. Compared to traditional epoxidation, the mechanism of lipase-catalyzed epoxidation based on the formation of peroxy fatty acids under the catalysis of lipase and the auto-epoxidation would take place under mild conditions [21].

The ring-opening reaction between the epoxy group and the amino group of the surface residues of protein could automatically take place under the mild conditions at room temperature [22]. Results in Table 1 indicated that an initial protein loading higher than 0.04 mg/cm^2 would not significantly improve the protein capacity of the metal carrier, due to its limited specific area. The maximum capacity of the stainless-steel net (mesh number of 30 M, fiber diameter of 0.15 mm, mesh opening size of 0.7 mm) for the protein was around $6.59 \text{ }\mu\text{g/cm}^2$. When the immobilized protein was changed to FAH (fatty acid hydratase from *Lactobacillus acidophilus*), the immobilized recovery and capacity (Table 1, line 5 and 6) were similar to that of the CALB lipase, which means that the method has a good universality for different enzymes.

Table 1. Influence of the initial protein loading on the capacity of stainless-steel net.

No.	Enzyme	Initial Enzyme Loading (mg/cm^2)	Immobilized Recovery (%)	Enzyme Capacity ($\mu\text{g/cm}^2$)
1	CALB	0.02	25.8 ± 2.2	5.16
2	CALB	0.04	16.5 ± 1.4	6.59
3	CALB	0.06	11.1 ± 1.2	6.66
4	CALB	0.08	8.3 ± 1.8	6.62
5	FAH	0.04	17.2 ± 1.6	6.89
6	FAH	0.06	10.1 ± 1.8	6.06
7	FAH on resin	5 mg/g	37.6 ± 2.3	1.88 mg/g

Contact angle changes were assessed to check the immobilization of the enzyme on the surface of stainless-steel materials. From the results of Figure 4, it could be found that the surface of the stainless-steel nets was totally hydrophobic after the acid etching. Oxidation treatment would improve the hydrophilicity of the metal surface due to the formation of $\text{FeO}_x(\text{OH})_y$, a kind of ferric oxide. Chelation with dopamine and grafting with oleic acid would increase the hydrophobicity of the metal surface based on the hydrophobic character of the benzene ring and alkyl chain. Finally, after the immobilization, it had a significant decrease of the contact angle. The size of the hydrophilic protein is much larger than the hydrophobic benzene ring and alkyl chain (FAH from *L. acidophilus* was 67.6 kDa), and the hydrophilic functional group on the surface of the protein molecule shows a strong hydrophilic energy, which led to the formation of a thin layer of protein covering the surface of metal carrier.

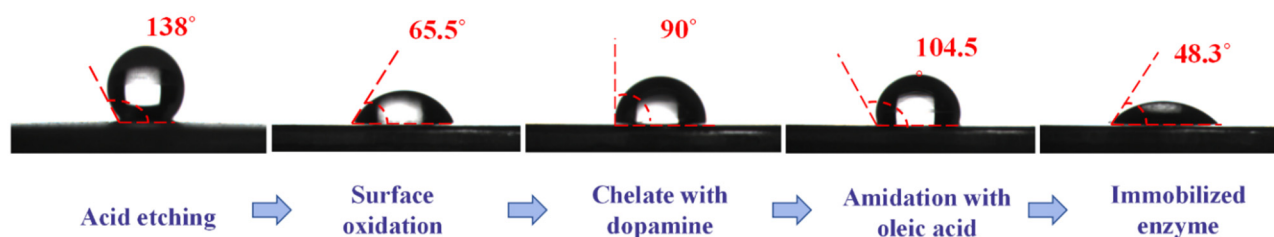


Figure 4. Contact angle changes during the process of immobilization.

From the characterization of the changing surface morphology during the immobilization, it was clear that acid etching significantly increased the specific area of the metal surface (Figure 5A,B). However, the following chelation and grafting treatment (Figure 5C) showed minor effects on the metal surface. The final morphology of immobilized enzymes (Figure 5D) showed that they were not uniformly dispersed on the surface of the support and that most of the enzymes were immobilized in the pore structures created by acid etching. Meanwhile, since the catalyst of Novozym 435 for the epoxy reaction was solid, it had less chance to have a ring-opening reaction with the epoxy group. From the SEM image of Figure 5D, there were no visible particles connected to the surface of metal materials.

It could be concluded that for the process of epoxy reaction, lipase was connected to the surface of metal materials.

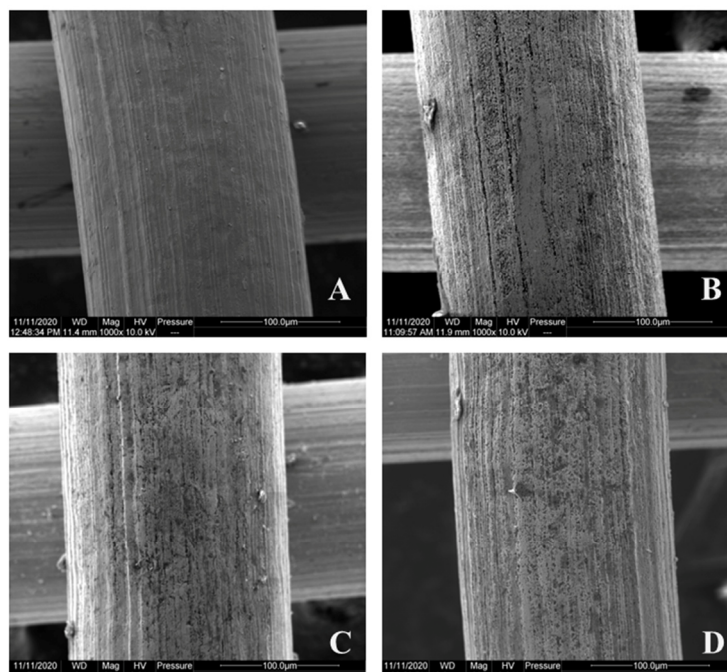


Figure 5. Surface morphology of a stainless-steel fiber after each treatment step (A) after NaOH washing; (B) after HCl etching; (C) after chelation with dopamine and grafting with oleic acid; (D) with lipase immobilized on its surface.

The kinetic parameters of the metal immobilization were also determined. The resin of D3520 was applied as a control to compare the performance of immobilization. D3520 resin is a co-polymer of cross-styrene-divinylbenzene, whose average pore diameter is 8.5–9.0 nm, and was widely applied for enzyme immobilization. The results of Table 2 indicated that the maximum reaction rate of the metal-immobilized enzyme was around two times higher than that of the immobilized enzyme supported by the granular porous carriers where the reduced pore structure lowers the internal diffusion resistance during the enzymatic reaction. It could not be avoided that covalent modification might cause some extent changes in the conformation of enzymes, which decreases the catalytic activity and leads to a lower V_{max} after attaching to the metal compared to the free enzymes. However, RPB could facilitate the mass transfer, and surface renewal increase the contact between substrate and enzyme which make up for the conformation change of enzymes and bring a higher reaction efficiency.

Table 2. Kinetic parameters of each immobilized enzymes.

Enzyme	Carrier	V_{max} ($\text{mmol}\cdot\text{mg}^{-1}\cdot\text{min}^{-1}$)	K_m (mM)
CALB lipase	Stainless-steel net	10.11	48.5
	D3520 Resin	5.01	15.5
	Free CALB	31.65	10.2
FAH	Stainless-steel net	0.95	25.5
	D3520 Resin	0.61	10.5
	Free FAH	9.57	8.6

Note: the details information for V_{max} and K_m calculation was provided in supplementary materials

2.2. Hydration of Linoleic Acid in the Meta-Immobilized FAH in a RPB Reactor

The hydratase-catalyzed synthesis of 10-hydroxy-*cis*-12-octadecenoic acid (10-HOA) (identified by $^1\text{H-NMR}$, results in supplementary materials) is a heterogeneous reaction, where the bio-catalytic reaction depends on the mass transfer efficiency. The catalytic results of the hydratase in the stirred tank reactor (STR) were selected as a comparison. As indicated in Figure 6a, the reaction in the RPB obtained a higher reaction rate and yield in the production of 10-HOA compared to that in the STR. It considerably shortened the reaction time and improved the conversion rate. Whereas a yield of 84.2% in 20 h was obtained in STR, the RPB yield exceeded 80% in 10 h under the same conditions in RPB with immobilized enzyme (both of metal and particle immobilized FAH). This was attributed to the higher collision probability in the RPB between the reaction substrate and the rotor packing, hence improving the mixing of oil and water phase substrates, increasing the contact area and enhancing the mass transfer between two phases. In addition, the metal immobilized enzyme has a faster conversion speed and better 10-HOA yield (92% for 24 h) compared to the porous particle immobilized FAH. The reduced diffusion resistance of the metal-immobilized enzyme significantly enhanced the catalytic efficiency.

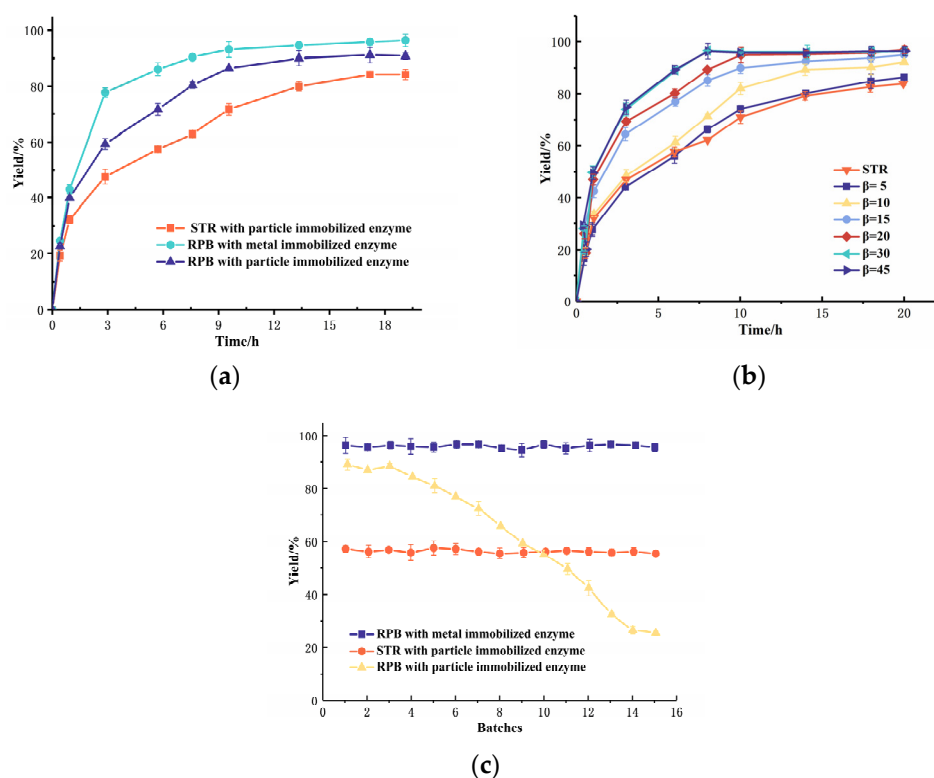


Figure 6. Comparison and optimization of hydration catalyzed by FAH in RPB; (a) Effect of the reactor type and enzyme morphology on the hydration reaction catalyzed by FAH; (b) Effect of centrifugal force factor on the hydration catalyzed by FAH; (c) Hydration reaction yield versus the lifetime of FAH.

2.3. Effect of the Centrifugal Force Factor in the Metal-Immobilized FAH Catalyzed Hydration Reaction

The centrifugal force factor β is a key parameter of the mass transfer in a RPB, which directly affected the mass transfer and diffusion. As shown in Figure 6b, the yield of 10-HOA increased with an increasing β . The equilibrium could be achieved in 8 h when β exceeded 30, and the yield exceeded 96%. Compared with the STR, the reaction time was considerably decreased and the yield was increased from 84.2% to 96.6%. Moreover, our earlier work [23] for the particle-immobilized enzyme demonstrated that the enzymes would quickly denature at $\beta > 20$ due to the occurring shear forces. However, with the

metal-immobilized enzymes, the β factor could increase up to 30, thus proving a higher shear force resistance of the enzyme and a hampered enzyme denaturation.

2.4. Determination of the Reusability of Immobilized Hydratase with RPB

Enzymes, immobilized on the metal surface, showed a high efficiency in the hydratase-catalyzed linoleic acid hydration reaction. The comparison and evaluation of the enzyme reusability in RPB, STR were performed. The hydratase immobilized on the metal surface showed the best enzyme stability and highest yield (Figure 6c). Compared with the STR results, the yield of metal-immobilized FAH in a RPB was increased from 60% to 98%, due to the higher mass transfer and lower diffusion limitations. The traditional porous particle-immobilized FAH achieved a good yield when used twice, but progressively decreased after 4 batches (10 h for each batch). Its half-life period appeared to be 9 batches. This was mainly attributed to the loss of enzyme activity caused by the shear forces. On the contrary, the yield of the metal-immobilized FAH applied in the RPB reactor still exceeded 90% after 15 batches (10 h for each batch), proving its positive impact on reducing both the internal diffusion restriction and mechanical damage during the reaction. The nano-enzyme immobilization has low reusability and stability [24]. This immobilization enhanced the shear resistance ability of the immobilized enzyme. These positive effects greatly improved the reaction efficiency and the enzyme lifespan.

3. Materials and Methods

3.1. Strains, Plasmids, and Chemicals

Escherichia coli Top10 and BL21 (DE3) were obtained from Tiangen Ltd. (Beijing, China). Expression vectors pET22b were purchased from Novagen (Darmstadt, Hessian Germany). The gene of fatty acid hydratase (*L. acidophilus*, NCBI Reference Sequence: WP_011254216.1) was synthesized by Inovogen Ltd. (Shenzhen, China), and the sequence was inserted into the plasmid pET22b (+) between the NdeI and HindIII restriction nuclease sites. Lipase CALB solution, and immobilized lipase Novozyme 435 was purchased from Novozymes Co., Ltd., (Beijing, China). The stainless-steel net with grade of 304, mesh number of 30 M, fiber diameter of 0.15 mm, and mesh opening size of 0.7 mm, was purchased from a local building materials market. Oleic acid, linoleic acid, decenoic acid, acrylic acid, 4-(4,6-Dimethoxy-1,3,5-triazin-2-yl)-4-methylmorpholinium chloride (DMT-MM) and other chemicals were purchased from TCI (Shanghai) Development Co., Ltd. (Shanghai, China). All reagents were of analytical grade.

3.2. Production of Fatty Acid Hydratase

A plasmid with the FAH gene was electro-transferred into *E. coli* BL21 (DE3), and then the transformants were cultured in LB medium at 37 °C until the OD₆₀₀ reached 0.8. Subsequently, an induction with 0.5 mM IPTG at 20 °C took place for 20 h. Finally, the cells were collected by centrifugation at 4 °C, 4000 rpm for 10 min, and the sedimentary cells were further disrupted by sonication (400 W, 15 min). The soluble expression of FAH was purified by a His-tag through Ni-NTA affinity chromatograph (see supplementary information).

3.3. Immobilization of Enzyme on the Stainless-Steel Carrier

3.3.1. Pre-Treatment of Metal Carrier

The metal carrier was washed with a NaOH solution (0.5 M) for 6 h to remove surface impurities, and then washed to neutrality using de-ionized water. The metal carrier was etched with HCl solution (0.5 M) for 12 h. Afterwards, it was washed to neutrality by de-ionized water again. It was subsequently oxidized by hydrogen peroxide (concentration of 20%, boiling for 1 h) or potassium permanganate (concentration of 0.75 M to 10 M, oxidation for 10 h), rinsed with de-ionized water and dried for further use.

3.3.2. Chelation with Dopamine

The pre-treated metal carrier was immersed in the dopamine hydrochloride solution and placed into a stirred reactor for 12 h (20 °C, 180 rpm, dark reaction). The wire mesh was rinsed with de-ionized water and dried. Then, the dopamine hydrochloride chelated wire mesh was obtained.

3.3.3. Amidation with Unsaturated Organic Acid

Acrylic acid, 9-decenoic acid, oleic acid, and linoleic acid were chosen as a linker, and all of these unsaturated organic acids was under the same treatment process to promote amidation reaction. The reaction time for each linker was the same. The unsaturated organic acids (200 µL) were dissolved in a NaOH solution (5 M), and diluted to a constant volume of 5 mL using water (pH 9.0). A DMTMM (1.2-fold molar weight to the unsaturated organic acid, 5 mL) solution was quickly prepared to prevent oxidation. The metal carrier was placed in the mixture of both solutions, and stored in darkness for 3 h. It was rinsed with deionized water and dried for further use.

3.3.4. Epoxy Reaction

Commercial immobilized lipase Novozym 435 was applied as catalyst for the epoxy reaction. The metal carrier grafted with unsaturated organic acids was submerged into a conical flask of n-hexane. n-Octanoic acid (1 mM), 30% H₂O₂ (0.4 mL/L) and Nov 435 lipase ($m_{\text{Nov 435}}:m_{\text{Fatty acid}} = 1:10$) were added into the flask, and left into a stirred reactor for epoxidation (15 °C, 200 rpm, 12 h). The carrier with branched epoxy structure was obtained after washing and drying.

3.3.5. Epoxy Ring-Opening for Enzyme Immobilization

The epoxy-treated metal net carrier was inserted into a conical flask containing the target enzyme in a phosphate buffer (pH 7.2, CPBS 2 mM). It was stirred for 12 h (15 °C, 180 rpm) for epoxy ring-opening. At the end of the reaction, the metal carriers were rinsed with phosphate buffer and dried. The metal-immobilized enzyme was obtained.

3.3.6. Macro-Porous Resin Immobilization of FAH

Macro-porous resin D3520 was applied for the adsorption immobilization of the enzyme. The immobilization condition involved adding 5 g of resin into 40 mL sodium phosphate buffer (100 mM, pH 7.2). Then, 100 mg FAH powder was added, and the mixture was stirred at 25 °C, 180 rpm for 24 h. After adsorption, the resin was separated and washed with sodium phosphate buffer.

3.4. Enzyme Immobilized Recovery Analysis for the Immobilization

The enzyme immobilized recovery was calculated by the following equation [25] according to BSA standards.

$$\text{immobilized recovery (\%)} = \frac{C_i - C_f}{C_i} \quad (1)$$

The protein concentration was determined by Bradford's Kaumas Brilliant Blue method (details listed in supplementary materials). C_i and C_f represent the initial and final protein concentrations, respectively, mg/L. The calculation method for enzyme capacity is listed in the supplementary materials.

3.5. Immobilized Lipase Catalyzed Synthesis of n-Octyl Laurate

The enzymatic esterification was applied to optimize the immobilization process. Metal-immobilized enzymes (2 cm² of metal carrier) and 3.5 mL substrates (lauric acid, n-octanol, 5 mM) were mixed in a 5 mL glass vial, and placed in a stirred reactor at 40 °C, 600 rpm, for 3 h. Samples were taken at regular intervals during the reaction process, and then measured by GC (GC-2010 plus, Shimadzu, Tokyo, Japan).

3.6. Characterization of Surface Structure and Properties of Immobilized Enzyme

A piece of stainless-steel fleece with an area of 0.2 cm² was applied for SEM analysis. The surface geometry was photographed by scanning electron microscopy (SEM, Sep 012020 type, Tokyo, Japan). The water contact angles of the metal materials were measured by an optical contact angle measuring instrument (DSA30S, Kruss, Germany).

3.7. Hydration of Linoleic Acid by Metal Immobilized FAH with a RPB Reactor

Parameters of the RPB reactor applied in this study were as follows: the radius of rotor was 35 mm, the length of rotor was 55 mm, and the radius of RPB shell was 75 mm.

For the hydration reaction, previous work has optimized FAH catalyzed hydration of linoleic acid with a stirred tank reactor [26]. Based on the previous work, the general hydration conditions for RPB were set as follows: 100 mL of 50 mM citrate phosphate buffer (pH 7.0), with 0.05% (v/v) tween 20, linoleic acid concentration of 10 g/L, 484 cm² metal-immobilized FAH (5.5 cm × 8.8 cm, rolled into 4 layers in the rotor) were applied for the catalyst, and the reaction temperature was 30 °C. The reaction conditions were the same except the kinds of immobilized enzyme, and the type of reactor. For each batch of reaction, the reaction lasts for 4 h.

The rotation factor β of the RPB reactor was set from 5 to 45, thus enabling checking of the mass transfer enhancement of RPB on the enzymatic reaction. The relationship of β with the parameters of rotor speed (v , rad/min), rotor radius (r , m), and the gravitational acceleration (g , m/s²) could be expressed by the following equation:

$$\beta = \frac{v^2 r}{g} \quad (2)$$

For the analysis of the hydration product, 5 mL of reaction liquid was taken, and 1 mL of ethyl acetate was added to the sample for extracting the hydroxy fatty acid from the water. After centrifugation at 5000 rpm, the ethylacetate solution was used for GC (Shimadzu 2010 plus) analysis. GC condition was as follow: capillary-column DB-1 ht (30 m × 0.25 mm × 0.10 μ m, Agilent Technologies, J&W scientific columns) was applied for analysis. Nitrogen was used as the carrier gas. The temperature of the injector was set at 380 °C. The initial temperature of the column was 80 °C, maintained for 1 min. Then the column temperature was increased to 280 °C at a ramp of 8 °C/min and maintained for 10 min. The contents of products were calculated with the method of area normalization. The concentration of the products was determined using the external standard method. All measurements were conducted in triplicate [26], detailed information for GC analysis was provided in supplementary materials. The data are shown as averages with their standard deviation of triplicate results.

4. Conclusions

The research results provided an effective strategy to immobilize enzymes on the surface of stainless-steel materials. The mechanism of this strategy was based on the chelate reaction between Fe³⁺ and the hydroxy group of dopamine. Furthermore, combined with the amidation of dopamine with oleic acid, epoxidation of unsaturated double bond, and epoxy ring-opening reaction by the enzyme, the enzyme could be immobilized on the metal surface through covalent bonding. Due to the excellent shear strength and resistant ability of the immobilized enzymes, this metal-immobilization method facilitated the direct immobilization of the enzymes on the metal packing net of the RPB reactor. Through a fatty acid hydratase immobilized on the stainless-steel packing net of RPB reactor, the advantage of this immobilization strategy combined with the mass transfer enhancement of RPB was proved. Under the operation condition of centrifugal force factor $\beta = 30$, the hydration conversion rate of 96% would be achieved after 8 h, compared to the yield of 60% in the STR, which was increased by nearly 38% higher. The application of this metal-immobilized enzyme considerably promotes the heterogeneous hydration reaction

at the oil-water interface, improves the reaction efficiency, and shortens the equilibrium time. Moreover, the stability of this metal-immobilized enzyme was also improved, and the conversion rate exceeded 90% after 15 batches. All the results indicated that this metal immobilization method, combined with the RPB reactor, not only increases the efficiency of enzymatic reactions, but also provides conditions of the mass transfer enhancement in other enzymatic heterogeneous reactions.

Supplementary Materials: The following supporting information can be downloaded at: <https://www.mdpi.com/article/10.3390/catal13121501/s1>, Figure S1: Standard curve of the BSA protein, Figure S2: Fitting curve of double reciprocal of concentration and rate of enzyme (a) CALB lipase on stainless-steel net (b) CALB lipase on D3520 Resin (c) FAH on Stainless-steel net (d) FAH on D3520 Resin, Figure S3: Gas Chromatography of 10-HOE (a) Standard Linoleic acid (b) reaction for 1-h (c) reaction for 2 h (d) reaction for 4 h (e) reaction for 10 h, Figure S4: SDS-PAGE result of FAH 1. FAH before His-tag purification; 2. FAH after first time of purification; 3. FAH after second times of purification; 4. FAH after third times of purification, Figure S5: Identification of the hydration product by $^1\text{H-NMR}$, Table S1: $^1\text{H-NMR}$ Signals and molecular Assignments for 10-hydroxy-*cis*-12-octadecenoic acid.

Author Contributions: R.Y. and J.X. performed the experiments, data curation, and wrote original draft. J.W. and D.L. contributed to investigation, writing—review and editing. F.W. conceived and designed the experiments. K.N. supervised all data and wrote the paper together with all authors. All authors have read and agreed to the published version of the manuscript.

Funding: This research was funded by National Natural Science Foundation of China (21978017, 21978020). The authors would like to thank for the above funding.

Data Availability Statement: The data presented in this study are available in article and supplementary material.

Conflicts of Interest: Author Juntao Xu was employed by the company Sinovac Life Sciences Co., Ltd. The remaining authors declare that the research was conducted in the absence of any commercial or financial relationships that could be construed as a potential conflict of interest.

References

1. Baeyens, J.; Kang, Q.; Appels, L.; Dewil, R.; Lv, Y.; Tan, T. Challenges and opportunities in improving the production of bio-ethanol. *Prog. Energy Combust. Sci.* **2015**, *47*, 60–88. [[CrossRef](#)]
2. Jeswani, H.K.; Chilvers, A.; Azapagic, A. Environmental sustainability of biofuels: A review. *Proc. R. Soc. A* **2020**, *476*, 20200351. [[CrossRef](#)] [[PubMed](#)]
3. Mohamad, N.R.; Marzuki, N.H.C.; Buang, N.A.; Huyop, F.; Wahab, R.A. An overview of technologies for immobilization of enzymes and surface analysis techniques for immobilized enzymes. *Biotechnol. Biotechnol. Equip.* **2015**, *29*, 205–220. [[CrossRef](#)] [[PubMed](#)]
4. Luqueño, F.F.; López-Valdez, F.; Pérez, G.M. *Bio and Nanoremediation of Hazardous Environmental Pollutants*; CRC Press: Boca Raton, FL, USA, 2023.
5. Schrimpf, M.; Esteban, J.; Rösler, T.; Vorholt, A.J.; Leitner, W. Intensified reactors for gas-liquid-liquid multiphase catalysis: From chemistry to engineering. *Chem. Eng. J.* **2019**, *372*, 917–939. [[CrossRef](#)]
6. Wang, Z.; Yang, T.; Liu, Z.; Wang, S.; Gao, Y.; Wu, M. Mass Transfer in a Rotating Packed Bed: A Critical Review. *Chem. Eng. Process.-Process Intensif.* **2019**, *139*, 78–94. [[CrossRef](#)]
7. Bach, C.; Yang, J.; Larsson, H.; Stocks, S.M.; Gernaey, K.V.; Albaek, M.O.; Krühne, U. Evaluation of mixing and mass transfer in a stirred pilot scale bioreactor utilizing CFD. *Chem. Eng. Sci.* **2017**, *171*, 19–26. [[CrossRef](#)]
8. Ahmed, S.M.R.; Phan, A.N.; Harvey, A.P. Mass transfer enhancement as a function of oscillatory baffled reactor design. *Chem. Eng. Process.-Process Intensif.* **2018**, *130*, 229–239. [[CrossRef](#)]
9. Prem, S.; Helmer, C.P.O.; Dimos, N.; Himpich, S.; Brück, T.; Garbe, D.; Loll, B. Towards an understanding of oleate hydratases and their application in industrial processes. *Microb. Cell Factories* **2022**, *21*, 58. [[CrossRef](#)]
10. Soto, D.; Girard, H.-L.; Le Helloco, A.; Binder, T.; Quéré, D.; Varanasi, K.K. Droplet fragmentation using a mesh. *Phys. Rev. Fluids* **2018**, *3*, 083602. [[CrossRef](#)]
11. Chen, Y.H.; Huang, Y.H.; Lin, R.H.; Shang, N.C. A continuous-flow biodiesel production process using a rotating packed bed. *Bioresour. Technol.* **2010**, *101*, 668–673. [[CrossRef](#)]

12. Garba, U. Study of the impact of the morphology of a G/L contactor on the hydrodynamics and mass transfer in an RPB: Application to the treatment of gases in an embedded process. In *Etude de L'incidence de la Morphologie d'un Contacteur G/L sur L'hydrodynamique et le Transfert de Matière Dans un RPB: Application au Traitement de Gaz Dans un Procédé Embarqué*; Institut National Polytechnique de Toulouse—INPT: Toulouse, France, 2023.
13. Zou, Y.; Wang, F.; Li, A.; Wang, J.X.; Wang, D.; Chen, J.F. Synthesis of curcumin-loaded shellac nanoparticles via co-precipitation in a rotating packed bed for food engineering. *J. Appl. Polym. Sci.* **2022**, *139*, e52421. [[CrossRef](#)]
14. Zhang, L.; Gao, H.; Zou, H.; Li, Y.; Chen, J. Rotating Packed Bed Technology for Polymer Synthesis via Cationic Polymerization. *AIChE J.* **2009**, *56*, 1053–1062.
15. Xu, J.; Liu, C.; Wang, M.; Shao, L.; Deng, L.; Nie, K.; Wang, F. Rotating packed bed reactor for enzymatic synthesis of biodiesel. *Bioresour. Technol.* **2017**, *224*, 292–297. [[CrossRef](#)] [[PubMed](#)]
16. Minier, M.; Salmain, M.; Yacoubi, N.; Barbes, L.; Méthivier, C.; Zanna, S.; Pradier, C.-M. Covalent Immobilization of Lysozyme on Stainless Steel. Interface Spectroscopic Characterization and Measurement of Enzymatic Activity. *Langmuir* **2005**, *21*, 5957–5965. [[CrossRef](#)]
17. Khan, M.F.; Kundu, D.; Hazra, C.; Patra, S. A strategic approach of enzyme engineering by attribute ranking and enzyme immobilization on zinc oxide nanoparticles to attain thermostability in mesophilic *Bacillus subtilis* lipase for detergent formulation. *Int. J. Biol. Macromol.* **2019**, *136*, 66–82. [[CrossRef](#)] [[PubMed](#)]
18. Roshdi, S.; Kasiri, N.; Rahbar-Kelishami, A. Deterioration effects of SiO₂ nanoparticles on the mass transfer in a single drop system with resistance in both phases. *Int. Commun. Heat Mass Transf.* **2022**, *139*, 106470. [[CrossRef](#)]
19. Ge, D.; Zeng, Z.; Arowo, M.; Zou, H.; Chen, J.; Shao, L. Degradation of methyl orange by ozone in the presence of ferrous and persulfate ions in a rotating packed bed. *Chemosphere* **2016**, *146*, 413–418. [[CrossRef](#)] [[PubMed](#)]
20. Orellana-Coca, C.; Camocho, S.; Adlercreutz, D.; Mattiasson, B.; Hatti-Kaul, R. Chemo-enzymatic epoxidation of linoleic acid: Parameters influencing the reaction. *Eur. J. Lipid Sci. Technol.* **2005**, *107*, 864–870. [[CrossRef](#)]
21. Zhang, X.; Wan, X.; Cao, H.; Dewil, R.; Deng, L.; Wang, F.; Tan, T.; Nie, K. Chemo-enzymatic epoxidation of Sapindus mukurossi fatty acids catalyzed with *Candida* sp. 99–125 lipase in a solvent-free system. *Ind. Crops Prod.* **2017**, *98*, 10–18. [[CrossRef](#)]
22. Mihailović, M.; Stojanović, M.; Banjanac, K.; Carević, M.; Prlainović, N.; Milosavić, N.; Bezbradica, D. Immobilization of lipase on epoxy-activated PuroLite® A109 and its post-immobilization stabilization. *Process Biochem.* **2014**, *49*, 637–646. [[CrossRef](#)]
23. Xu, J.-T.; Liu, C.-S.; Wang, M.; Nie, K.-L.; Deng, L.; Shao, L.; Wang, F. An Effective Biocatalytic Reactor–Rotating Packed Bed Applied in Hydrolysis Reactions. *Ind. Eng. Chem. Res.* **2017**, *56*, 1349–1353. [[CrossRef](#)]
24. Razzaghi, M.; Homaei, A.; Vianello, F.; Azad, T.; Sharma, T.; Nadda, A.K.; Stevanato, R.; Bilal, M.; Iqbal, H.M.N. Industrial applications of immobilized nano-biocatalysts. *Bioprocess Biosyst. Eng.* **2022**, *45*, 237–256. [[CrossRef](#)] [[PubMed](#)]
25. Wang, M.; Qi, W.; Jia, C.; Ren, Y.; Su, R.; He, Z. Enhancement of activity of cross-linked enzyme aggregates by a sugar-assisted precipitation strategy: Technical development and molecular mechanism. *J. Biotechnol.* **2011**, *156*, 30–38. [[CrossRef](#)] [[PubMed](#)]
26. Nie, K.; Lu, D.; Sun, B.; Fang, Y.; Ning, Z.; Wang, M. Enzymatic hydration of linoleic acid followed with selective chain cleavage for biofuels and biomaterials production. *J. Biobased Mater. Bioenergy* **2020**, *14*, 723–731.

Disclaimer/Publisher's Note: The statements, opinions and data contained in all publications are solely those of the individual author(s) and contributor(s) and not of MDPI and/or the editor(s). MDPI and/or the editor(s) disclaim responsibility for any injury to people or property resulting from any ideas, methods, instructions or products referred to in the content.